

A New Failure Criterion for Laminated Safety Glass

Christian Alter¹, Stefan Kolling¹, Jens Schneider²

¹ TH Mittelhessen, Institute of Mechanics and Materials, Wiesenstraße 14, 35390 Gießen

² TU Darmstadt, Institute of Structural Mechanics and Design, Franziska-Braun-Straße 3, 64287 Darmstadt

1 Abstract

The prediction of the head injury criterion (HIC) for pedestrian protection in automotive applications is still a great challenge. In particular, the simulation of the head impact on windshields requires a reliable FE-modelling technique as well as predictive material laws including the constitutive behaviour up to fracture. In the present work, a new non-local failure criterion based on fracture mechanics is presented for laminated safety glass under low velocity impact. The model is implemented as a user defined material model for shell elements in LS-DYNA. In order to represent the stress intensity in the vicinity zone of a crack tip, a mixture of the element erosion technique and a decrease of strength in the direction of cracks is considered. By that there is no need to determine the current stress intensity factor. The used failure prediction is very similar to a major stress criterion whereby the fracture strength depends on the stress rate and, in addition, on the fracture state of the next neighboring elements. The basic strength is derived from the first region of the crack-velocity dependency which is approximated by an empirical power law. The reduction of element strength in crack direction depends on the element size which allows the use of a regular, coarse mesh. Experimental results of head impact tests under different configurations are used for the validation of the present model.

2 Introduction

According to ECE R43, the windscreen must be designed to reduce possible injuries in the case of fracture. Additionally, the head impact test on windscreens regulated by international standards as the EC 78/2009 as well as in international safety ratings like the Euro NCAP, JNCAP and KNCAP has to be performed. In order to avoid fatal injuries for pedestrians, the head injury criterion (HIC) and the head performance criterion (HPC), respectively, has to be fulfilled. Therefore, a model of the human head gets shot on the windscreen with an initial velocity of 9.7 ± 0.2 m/s after the EC 631/2009. During the impact, the transversal acceleration components get measured in the center of gravity of the impactor. These accelerations are used to compute the dimensionless HIC value by

$$HIC = \left[\frac{1}{t_2 - t_1} \int_{t_1}^{t_2} a_{res} dt \right]^{2.5} (t_2 - t_1). \quad (1)$$

Thereby a_{res} is the resultant acceleration in unity of gravity and the time values t_1 and t_2 have to be chosen in such a way, that equation (1) gets maximized. To avoid fatal injuries, certain critical limits may not be exceeded by the dimensionless HIC value. The limits are defined in the different testing standards, for example 1000 in the EG 78/2009 and in a range between 650 for full score and 1700 for zero score in the Euro NCAP testing protocol. While this procedure has a monitoring function in the EC 78/2009 only, it is an inherent part of the rating tests.

Numerous modelling and simulation techniques for laminated safety glass can be found in the literature. From single multilayer shell models [1] over two coincident shell models [2,3,4], solid models [5], combined solid-shell models [7,8] to three layered shell models [9] among many other examples [6]. In particular, Pyttel et al. [9] proposed a promising failure approach for laminated glass, which will be discussed later. However, the prediction of the HIC-Value in advanced is still an open problem in crash simulation. The implementation of a reliable material model and a suitable failure criterion is still of great interest for industrial application.

In the present paper, a discretization method is shown which is capable to represent the deformation of the elastic range until first failure under low velocity impact loads [17]. The prediction of the HIC value with commonly used failure criteria is discussed as well as the properties of these models. Additionally, an alternative failure approach for shell elements is introduced and the results of the acceleration curves and the fracture pattern are compared to the other models.

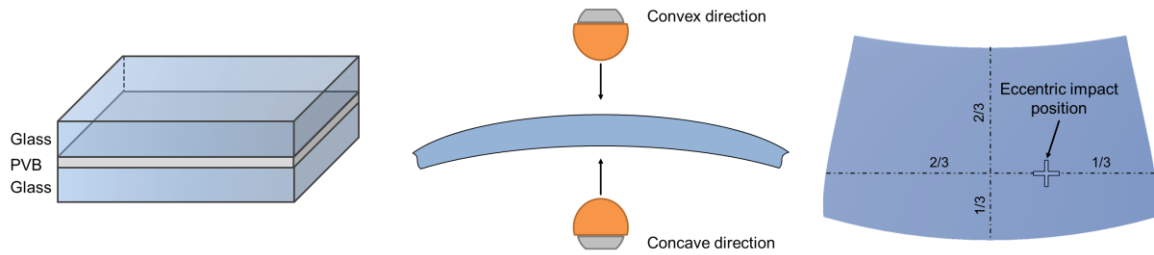


Fig. 1: Left: Composition of laminated glass. Middle: Definition of the convex and the concave impact direction. Right: Impact position for the eccentric experiment.

The presented new failure criterion is based on an empirical power law for the crack velocity to determine the rate depending fracture strength and uses an element size depending decrease of strength in the direction of crack propagation instead of an increase of the stress tensor near the crack tip. The procedure of strength reduction in the direction of the crack is similar to ***MAT_ORIENTED_CRACKS**, which is available in LS-DYNA, though for element type 1 only.

3 Laminated Glass

The general structure of windshields consists of at least two layers of glass which are bonded together by a viscoelastic interlayer of polyvinylbutyral (PVB) which is defined in the European Standard ECE R43 as laminated glass, see left-hand side of fig. 1. A reason for using laminated glass in the automobile industry is the behavior of the broken laminate, the so-called post breakage behavior. If one or both glass plies fail, the splinters remain on the interlayer. Occupants and pedestrians are thus protected from flying splinters and injuries can be avoided. Additionally, the broken laminate is still capable to transmit forces and bending loads and the interlayer is still capable to transmit tensile loads up to a large strain. While the basic constitutive law of glass is a simple linear elastic one up to failure, the fracture behavior is more complex and needs a fracture mechanical point of view. The strength of glass strongly depends on the stress rate and the size and position of initial flaws, e.g. micro cracks. Fast fracture in glass occurs if the stress intensity

$$K_I = \sigma_n Y \sqrt{\pi a} \quad (2)$$

with the crack opening stress σ_n , the crack depth a and a geometry factor Y reaches or exceeds the fracture toughness of glass which is in a range between approximately $0,75 \text{ MPa(m)}^{0.5}$ and $0,85 \text{ MPa(m)}^{0.5}$. Equation (2) can be used to determine the “inert strength” which indicates the maximum load limit. The stress rate dependency is a consequence of the so called “subcritical crack growth”, which leads to crack propagation effects below the inert strength [14]. Due to a probabilistic distribution of the size and position of the initial flaws, the failure strength scatters considerably. This additionally leads to a difference in strength between the edge [15, 16] and the surface of a glass plate [10]. Both effects can be seen in KOLLING et al. [2], where impact test under different loading rates were performed on the considered screens and the fracture strength was determined at the position of the initial failure. A normalized Weibull distribution [11] is shown in fig. 2 for the strength of the glass at the edge in comparison to the strength at the surface under quasi static and dynamic loading conditions.

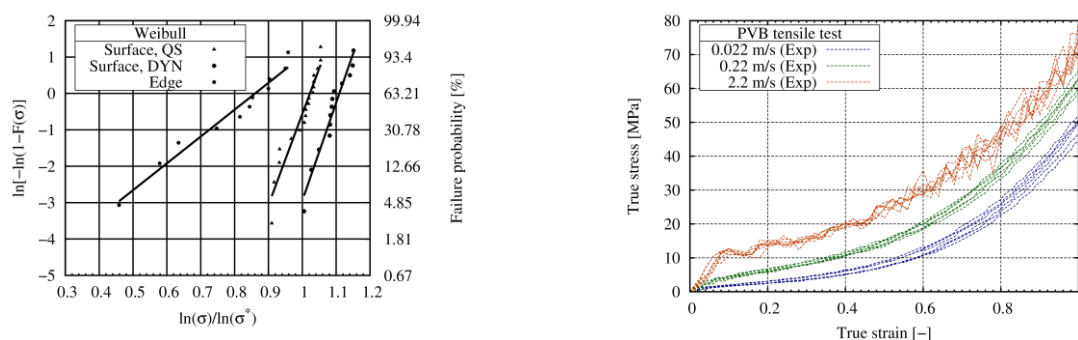


Fig. 2: Left side: Weibull distribution of the fracture strength of the edge and of the surface under different impact velocities, [2]. Right side: Tensile tests on PVB under different velocities, [2].

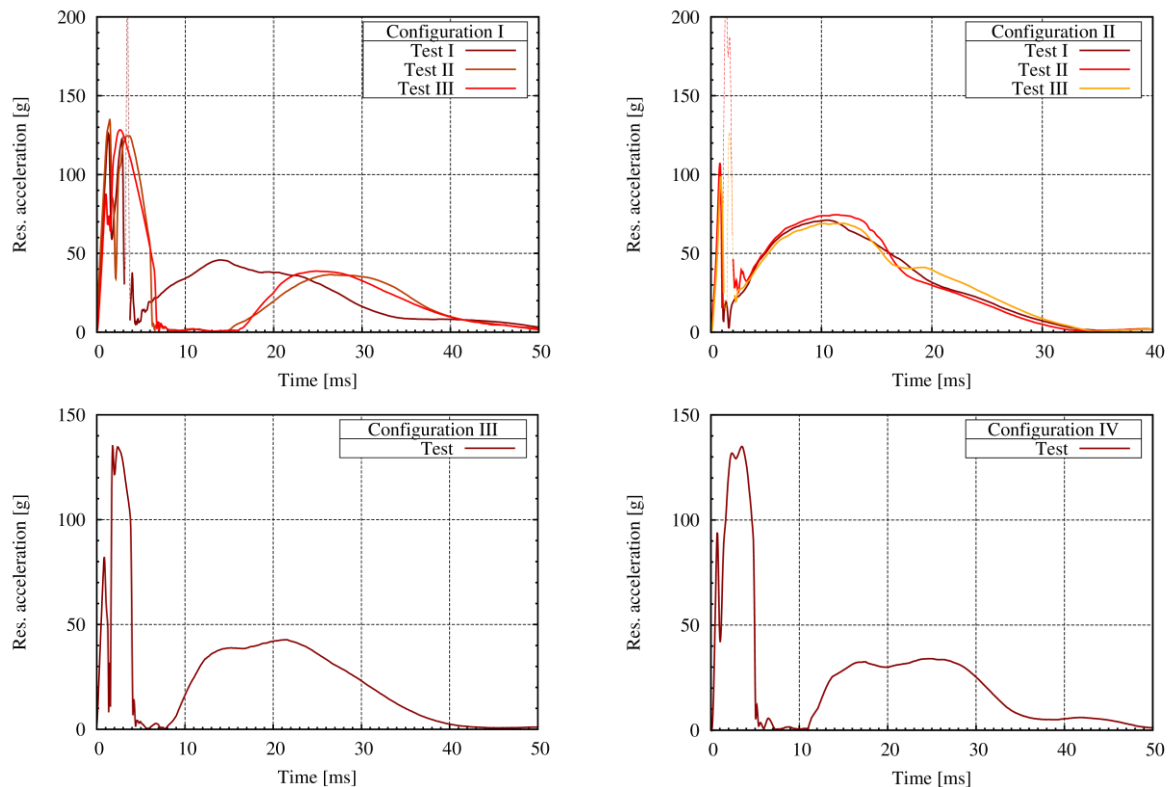


Fig.3: Resultant accelerations under different boundary conditions.

The PVB interlayer basically is a strongly nonlinear viscous hyperelastic material, see left-hand side of fig. 2 where tensile tests are shown for different velocities. Because of its very large strain at failure there is usually no failure of the interlayer unless the interlayer is damaged by some splinters.

4 Experiments

Dynamic head impact test under different boundary conditions were performed and an overview is given in tab. 1. The used screens consist of two layers of 1.8 mm float glass with a PVB interlayer of 0.76 mm and were tested in the convex (configuration I) and concave (configuration II) direction, see fig. 1. In order to get similar boundary conditions as in real car situations, the screens were glued on a wooden frame by a polyurethane adhesive. Each direction has been tested at the center position three times. The results of the measured accelerations are shown in fig. 3 at the top of the left side for the convex and at the right side for the concave direction. In the convex direction, a first peak with a large spread defined by the initial failure is followed by a distinctive second area of high acceleration. One test shows an extreme additional peak, dashed red lines. A more accurate analysis shows that this peak originally has a negative sign and so it is assumed that this is a measurement error due to unphysical behavior. In the concave direction, the initial peak also is followed by a second, relatively high acceleration peak in two of three tests, dashed lines. The second peak shows the same negative sign as in the convex test. So, it is not clear, if this peak exists at all. After a nearly complete missing of the acceleration, because of a contact loss between the impact model and the screen, a region of a smooth acceleration occurs, the so-called post breakage behavior. Additionally, an eccentric test in convex direction (configuration III), fig. 1 (right), and a test in the convex direction at the center position with a glass layer thickness of 2.1 mm (configuration IV) have been carried out. The resultant accelerations are shown in fig. 3 at the bottom of the left side for configuration III and at the right side for configuration IV. The behaviors of the accelerations are similar to the convex test at the center position with 1.8 mm glass.

The fracture patterns of the tests are shown in fig. 4. While the fracture pattern in the convex experiments cover a wide area of the glass surfaces and consists of radial and nearly oval circumferential cracks, the fracture pattern in the concave direction is more concentrated near the impact point. It also consists of radial cracks and circumferential cracks, which are rather circular in comparison to the convex direction.

Table 1: Definition of the testing configurations.

Configuration	Glass thickness [mm]	Impact position	Direction	Number of tests
I	1.8	centric	convex	3
II	1.8	centric	concave	3
III	1.8	eccentric	convex	1
IV	2.1	centric	convex	1

5 Discretization and Constitutive Relation

5.1 Meshing

The chosen discretization consists of two layers of shell elements for the glass plies and a solid layer for the PVB, fig. 5. The transmission of the shear stress components is realized by a coincident coupling of the shell and the solid elements. The physical composition of the laminate is modelled by a shifting of the physical and the contact thickness of the shell elements by a half of the shell depth. The shifting can be done easily in LS-DYNA by the CNTCO and the NLOC flag. The edge length of the shell elements is approximately 10 mm, which is a commonly used mesh size in practical applications. In order to get independent of the element shape, a regular mesh is used. The wooden frame and the adhesive bonding are modeled by solid elements. The connection between the laminated glass and the bonding gets realized via null-shells with a `*CONTACT_TIED_SHELL_EDGE_TO_SURFACE_BEAM_OFFSET` contact card. An explosive drawing of the entire model is shown in fig. 5. The FE-model of the head impactor, validated in [12,13], has been provided by Lasso Ingenieurgesellschaft mbH.

5.2 PVB interlayer

For the constitutive behavior of the PVB interlayer the material model `*MAT_HYPERELASTIC_RUBBER` is used. The stress response is derived by superposing the basic hyperelastic and the rate depending viscous stresses. For the hyperelasticity, a polynomial approach of the strain energy density function is used. The viscous part is modelled by a Prony series of four Maxwell elements in parallel. The identification of the parameters is outlined by RÜHL in [2] by fitting uniaxial tensile test under different velocities. A comparison of the measured and calculated curves and additionally a list of the chosen input parameters is shown in fig. 6.

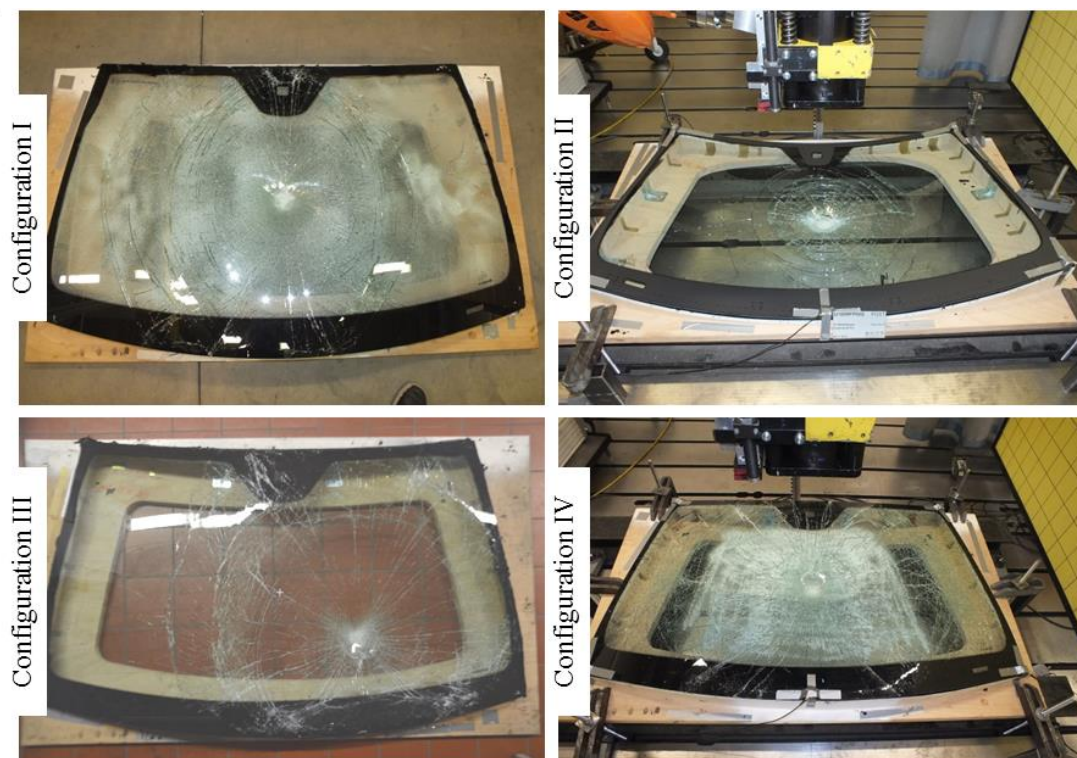


Fig.4: Fracture pattern of the different experiments.

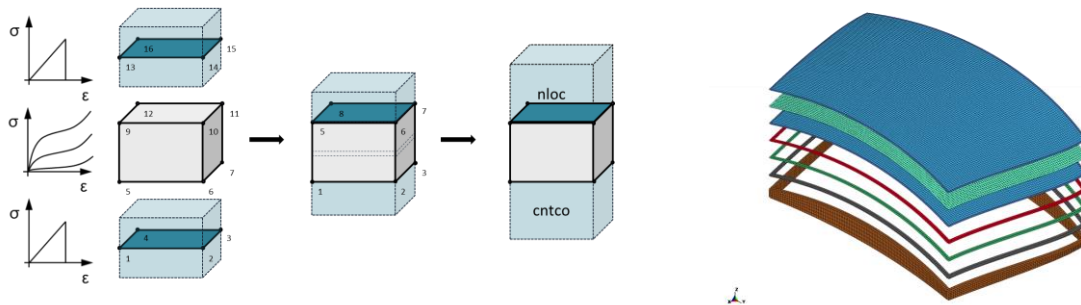


Fig.5: Left side: Coincident coupling of the shell elements for glass and the solid elements for the PVB interlayer. Right side: Explosive drawing of the entire model.

5.3 Adhesive bonding

The polyurethane adhesive as a part of the elastic bedding is simplified by a strain rate depending spring model. Therefore, the material model ***MAT_FU_CHANG_FOAM** is used. The input curves under constant strain rates are generated by tensile and compression tests under different velocities. The results are used to generate a stress–strain–strain rate surface. The quasistatic stress-strain relation is fitted by a modified Hill energy density function for high compressible materials and the rate dependency is considered by a Johnson–Cook approach. The results of the fitting procedure are shown in fig. 7.

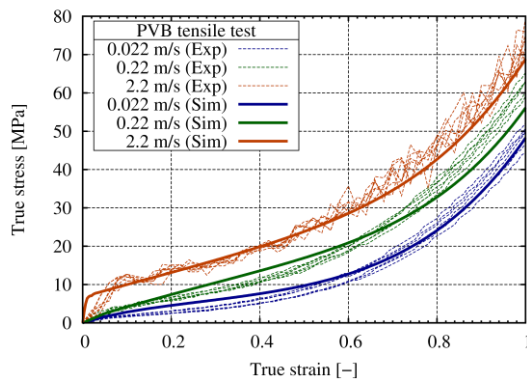
5.4 Glass

The behavior of glass is modelled by a simple linear elastic material model until failure. Therefore, the mechanical properties of the European standard DIN EN 572-1 are used with a Young’s modulus of 70 GPa, a Poisson ratio of 0.23 and a density of 2.5 kg/m³. In the present paper, three different failure approaches are used: A major strain criterion, a non-local criterion according to PYTTEL et al. [9], named PLC, and the new non–local approach. The major strain as well as the PLC criterion are applied by an additional ***MAT_ADD_EROSION** card while the new non–local approach is not implemented yet and only available as a user defined material model.

6 Validation

6.1 Major strain criterion

The major strain criterion in combination with the element erosion technique is used to reproduce failure which occurs if the current major strain reaches or exceeds a critical value. In order to obtain comparable results, each simulation was performed by a maximum major strain value of $\epsilon_{maj} = 0.004$. The results of the simulation in comparison to the measured curves are shown in fig. 8. On the one hand, the first failure of the glass plates is predicted in an acceptable way for the different configurations. To reproduce the second region of high acceleration, an increase of the strength is required, but this will not be capable to predict the whole range due to a decrease of the major strain in the region of decreasing acceleration.



Parameter	Value
C10	0.241E-03
C01	0.206E-02
C11	-0.23E-03
C20	0.404E-03
C02	0.182E-04
C30	-0.63E-05
G1	0.6845
G2	0.003
G3	0.00478
G4	0.0003
β_1	30.84
β_2	0.01
β_3	0.011
β_4	2.0

Fig.6: Validation of tensile tests on PVB under different velocities with ***MAT_HYPERELASTIC_RUBBER** together with the chosen input parameters.

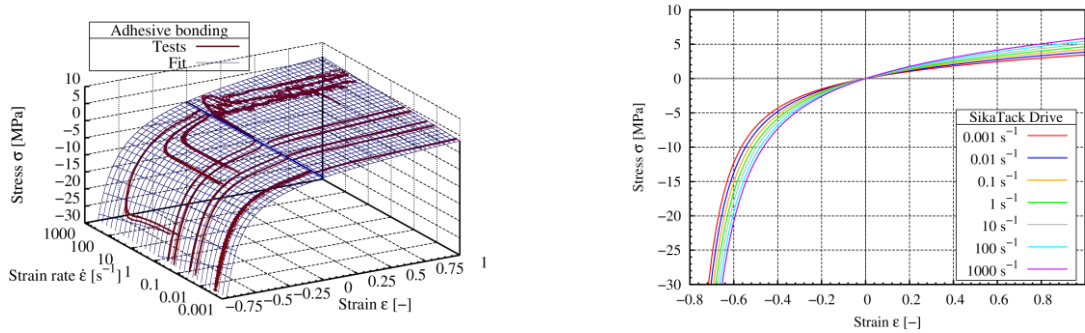


Fig.7: Generation of the constant strain rate input curves for the adhesive bonding from tensile and pressure test under different velocities.

Nevertheless, in contrast to an increase of the maximum strain, a strongly reduction would be needed to obtain a realistic post breakage behavior. The need of a reduction of the maximum major strain can also be seen in the simulated fracture pattern, which shows an underestimation of the real fracture pattern. Fig. 9 shows exemplarily the fracture pattern of the simulation of configuration I at the left and for configuration II at the right side.

6.2 PLC-Criterion

Pyttel et al. [9] proposed a non-local approach in order to avoid the disadvantages of the classical failure models as described in the previous section. Therefore, they used a so-called hybrid failure criterion. The main criterion for the element erosion is a major stress criterion, which is not considered until an energy based threshold criterion in a defined area is fulfilled. Therefore, the windscreen gets impacted until a major stress condition is fulfilled by an element. This element becomes the center of a circle with a predefined radius r . In this circle, the strain energy is computed until a critical energy is reached. After the energy criterion is fulfilled, the major stress criterion is activated for element erosion in the whole windscreen. This method allows the use of a low fracture strength for the post breakage behavior while the initial peak may be exceeded due to the energy criterion. Based on different experiments, PYTTEL et al. recommended the parameters $\sigma = 60$ MPa for the fracture strength, $r = 210$ mm for the radius and $E = 22.3$ J for the critical energy. The results of the simulation with the recommended values are shown in fig. 10 for the different testing configurations.

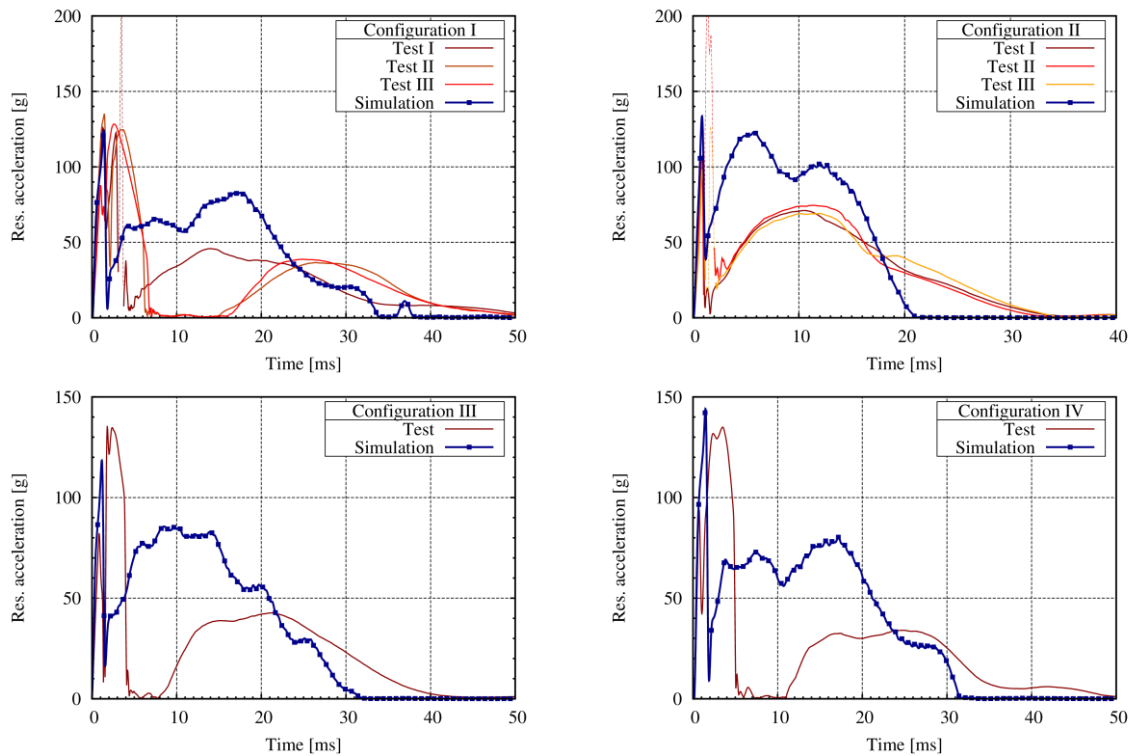


Fig.8: Comparison of the resultant acceleration of the tests and the simulations for the major strain criterion.

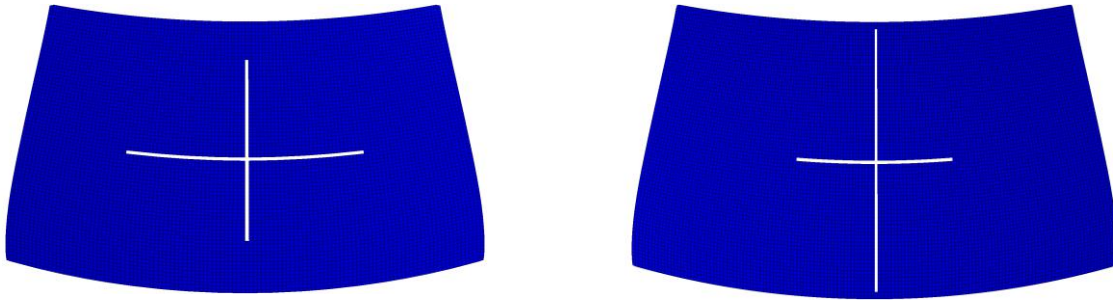


Fig.9: Fracture pattern of the simulation for the major strain criterion.

As can be seen, the PLC-Criterion significantly improves the prediction of the resultant acceleration in comparison to the classical approach. Additionally, the fracture pattern in fig. 11 is more realistic. Nevertheless, there are some disadvantages in the model related to the physical behavior. The crack growth is not physically described and the input parameters are abstract as well as empirical based. Consequently, the first fracture is skipped and the crack propagation differs from the experiment, where the origin of the initial crack is under the impact position [17] and propagates through the plates in a radial manner while the circumferential cracks arise later. In the simulation, fracture occurs under the impact position and simultaneous the circumferential cracks occur.

6.3 A new failure approach

The PLC approach significantly improves the reliability of the simulation of the head impact on windscreen. Due to the disadvantages of the criterion, an alternative approach was implemented as a user defined material model in LS-DYNA. The predictions of the fracture strength as well as the crack propagation are solely based on physical phenomena using fracture mechanics. The use of the new failure approach requires the specification of the initial crack lengths at the edge and at the both surfaces of a glass ply. Additionally, the material depending strength parameters K_{IC} and K_{TH} and environment dependent crack growth parameters can be modified but recommended values for glass are available in literature as used in the present work. These parameters are $K_{IC} = 0.75 \text{ MPa(m)}^{0.5}$ for the fracture toughness, $K_{TH} = 0.25 \text{ MPa(m)}^{0.5}$ for the crack growth threshold and $n=16$ and $v=0.006 \text{ m/s}$ for the first region of slow crack growth regime.

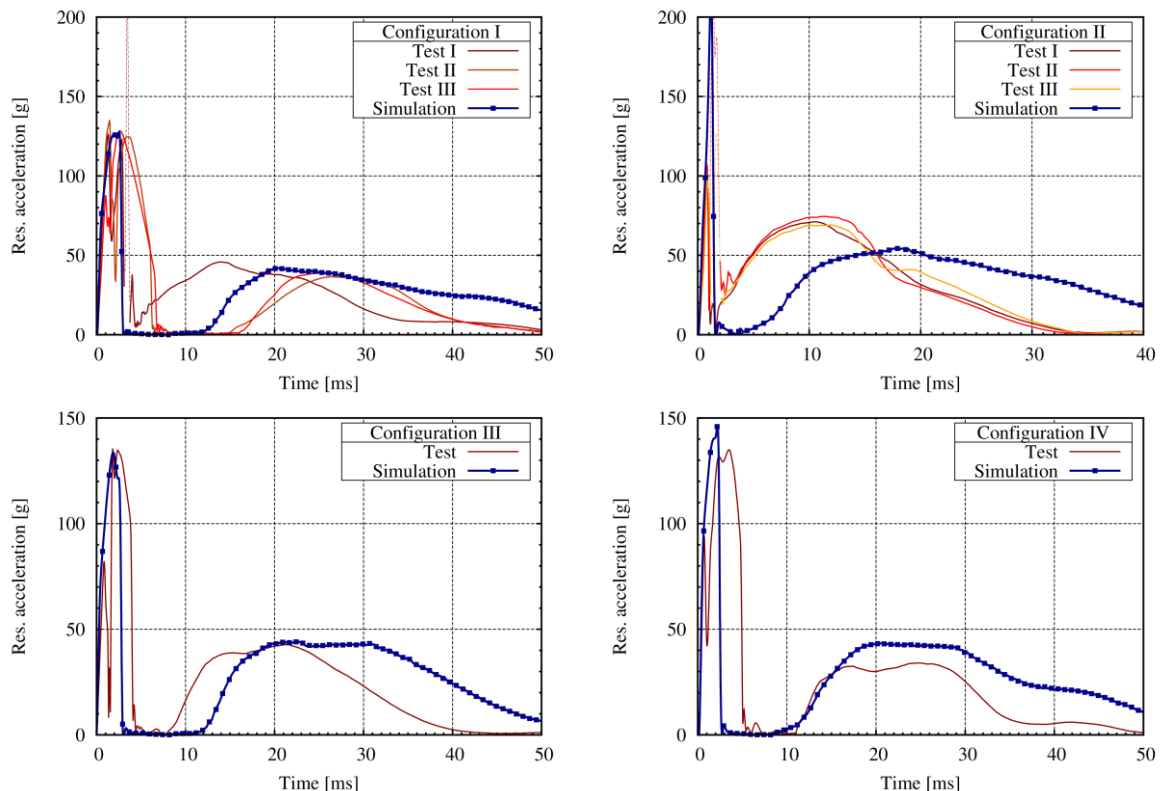


Fig.10: Comparison of the acceleration curves of the test and the simulation for the PLC criterion.

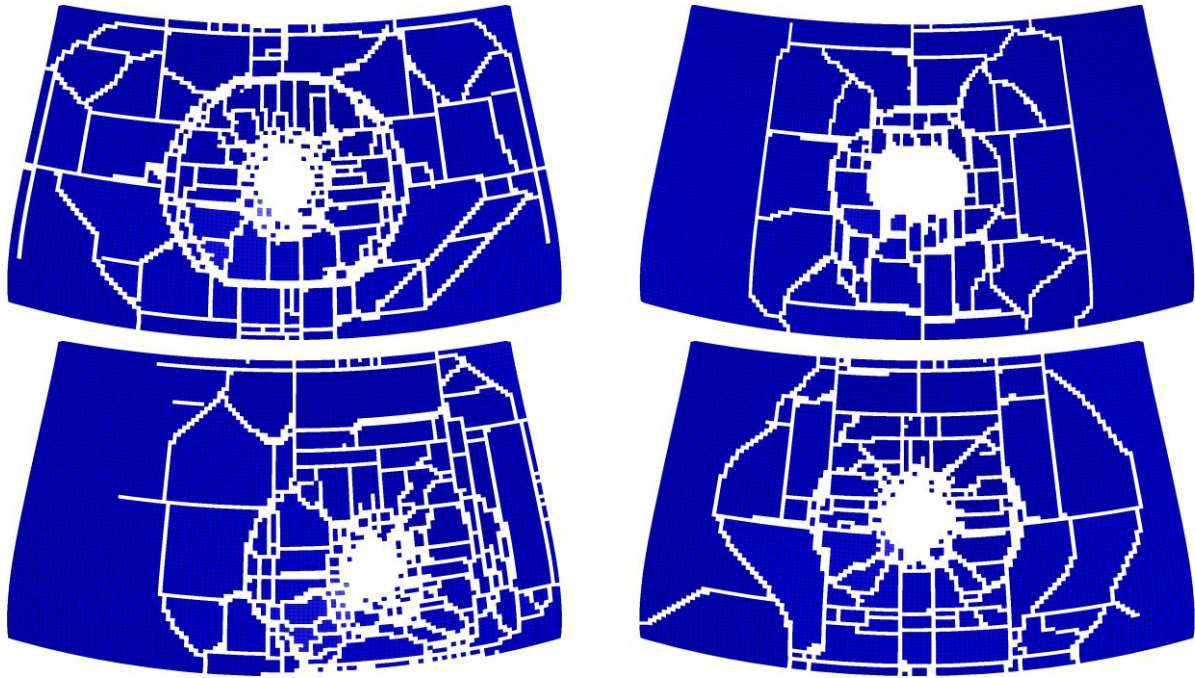


Fig.11: Fracture pattern of the simulation for the PLC criterion.

The current fracture strength depends on the one hand on the stress rate and additionally on the fracture state of the neighboring elements. In case of an element failure, the information is transmitted to the element in perpendicular direction to the failure causing major stress which leads to an element size depending decrease of the current strength. Fig. 10 shows the comparison of the measured and the calculated acceleration curves. As can be seen, the initial fracture as well as the second region of high acceleration can be described very well by the model. Moreover, also the post breakage behavior is approximated quite well.

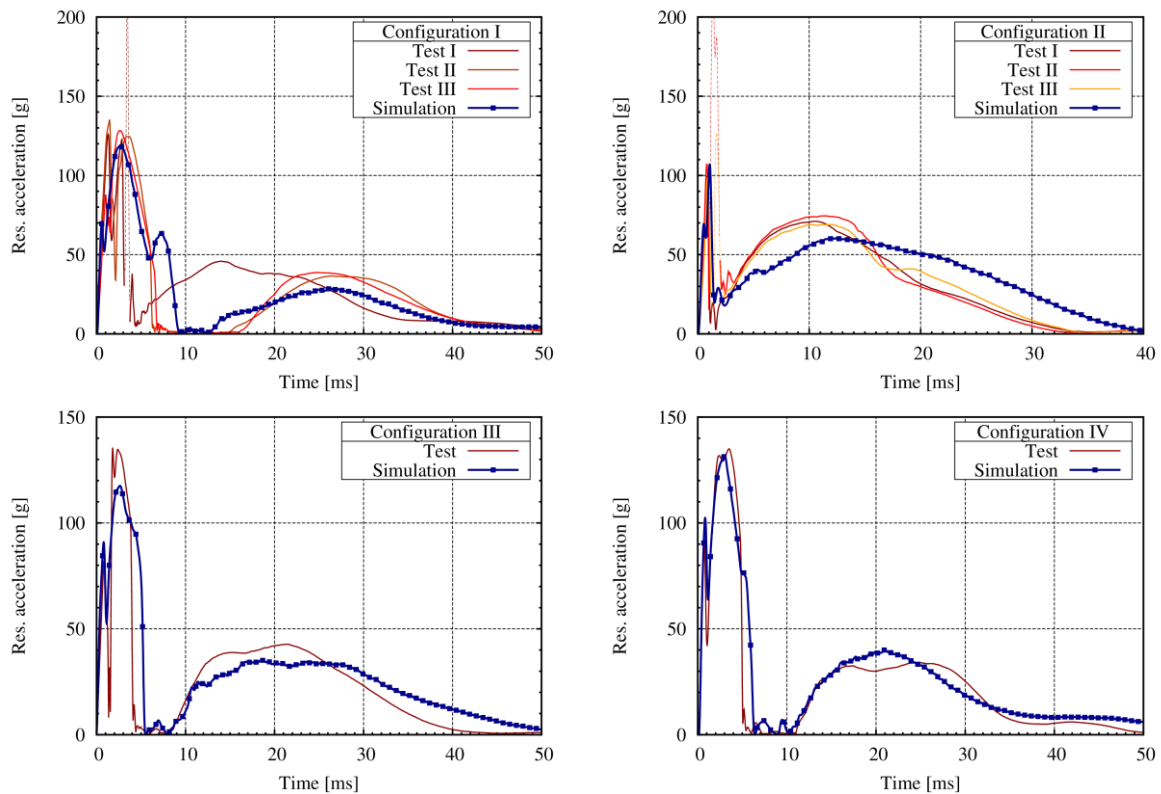


Fig.12: Comparison of the resultant acceleration of the test and the simulation with the new criterion.

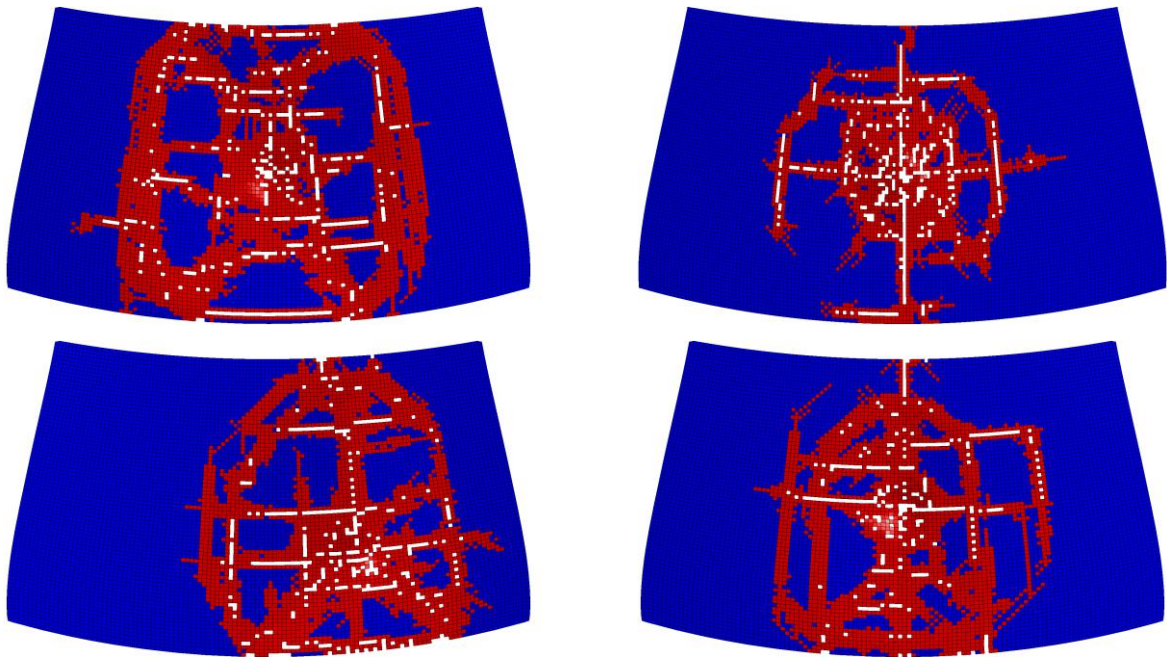


Fig.13: Fracture pattern of the simulation for the new criterion criterion.

The fracture patterns are shown in fig. 11. The red colored elements indicate the present of cracks in this area. As can be seen, the fracture shape gets more realistic and, in addition, the crack in the simulation starts under the impact point if the initial acceleration peak is reached, growths then through the glass and circumferential cracks occur at the end of the second acceleration region.

6.4 Overall comparison of HIC, t_1 and t_2

Due to a quantitative comparison of the different failure models, the measured and calculated HIC values and the corresponding time intervals t_1 and t_2 are shown in fig. 14. A comparison of the HIC values shows, that the PLC and the new failure criteria are both near the measured values while the major strain criterion significantly overestimates the results. The PLC criterion tends to underestimate the HIC value but booth, the PLC and the new criterion, deliver useful results. The prediction of the t_1 value is nearly the same for all three criteria, while a wide scatter can be seen for t_2 . In convex direction, the major strain criterion is far away from the measured values while in concave direction it is in the measured range. The PLC and the new criterion deliver similar results in the convex direction while both models overestimate the time value in concave direction.

7 Summary

The present work showed a comparison of a classical major strain criterion, a non-local criterion from PYTTEL et al. (PLC-criterion) and a new, physically based non-local failure criterion for low velocity impact simulation on laminated glass. While the PLC uses a maximum principal stress, a critical energy and a critical radius as input parameters, the parameters of the new model are solely motivated by linear elastic fracture mechanics. Additionally, the new approach takes care about the influence of the stress rate on the fracture strength and about the crack velocity in glass for crack propagation.

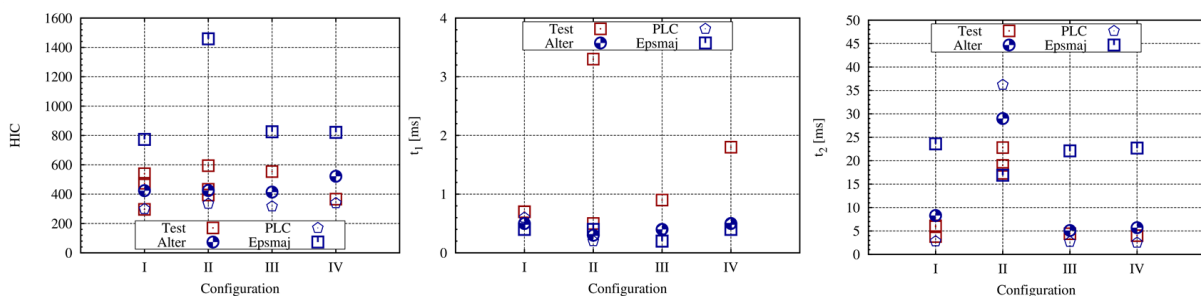


Fig.14: Comparison of the HIC-Values and the corresponding time intervals t_1 and t_2 .

Thus, the prediction of the initial failure and the crack propagation is improved significantly by the new model and it delivers a qualitative better result of the fracture depending characteristics of the acceleration curve. A quantitative comparison shows that the use of the classical failure approach in combination with a coarse mesh is not suitable while the non-local approaches deliver useful results. A comparison of the both non-local criteria shows, that the quantitative values are in a comparable order. In order to validate the universality and usability of the different models, a comparison under different load cases with a variety of the impact velocity and boundary conditions are topics of further investigation. Additionally, further studies must be performed with respect to the strength decreasing function in dependence on the element size and the mesh sensitivity of the crack propagation.

8 Acknowledgement

This research project named 17N1111 dealing with "Experimentelle und numerische Untersuchungen von Windschutzscheiben unter stoßartiger Belastung zur Verbesserung des Fußgänger- und Insassenschutzes" is supported by the German Federal Ministry for Economic Affairs and Technology. We would like to thank them for this sponsorship. The work is carried out in cooperation with "Forschungsvereinigung Automobiltechnik e.V. (FAT)".

9 Literature

- [1] Konrad, M., Gevers, M.: "Optimierung eines Verbundsicherheitsglasmodells für Kopfaufprall auf Windschutzscheibe". 9. LS-DYNA Anwenderforum, Bamberg, 2010.
- [2] Kolling, S., Du Bois, P.A., Fassnacht, W.: "Numerical Simulation of a Windshield for Crashworthiness". Proceedings of the 2nd LS-DYNA Forum, Bad Mergentheim, Germany, V33, 2002, 1–10.
- [3] Du Bois, P.A., Kolling, S., Fassnacht, W.: "Modelling of Safety Glass for Crash Simulation". Computational Materials Science, 28(3/4), 2003,675–683.
- [4] Timmel, M., Kolling, S., Osterrieder, P., Du Bois, P.A.: "A finite element model for impact simulation with laminated glass". International Journal of Impact Engineering, 34(8), 2007,1465-1478.
- [5] Thompson, G. M., Kilgur, A.: "Detailed Windscreen Model for Pedestrian Head Impact". 9. LS-DYNA Anwenderforum, Bamberg, 2010.
- [6] Kolling, S., Schneider, J., Gebbeken, N., Larcher, M., Alter, C., Kuntsche, J.: "Deformations- und Bruchverhalten von Verbundsicherheitsglas unter dynamischer Beanspruchung", Stahlbau, 81, 2012, 219-225
- [7] Sun, D.-Z., Andrieux, F., Ockewitz, A., Klamsner, H., Hogenmüller, J.: "Modeling of the Failure Behaviour of Windscreens and Component Tests". 4. LS-DYNA Anwenderforum, Bamberg, 2005.
- [8] Kolling, S., Alter, C., Rühl, A.: "Experimentelle und numerische Untersuchungen von Windschutzscheiben unter stoßartiger Belastung zur Verbesserung des Fußgänger- und Insassenschutzes". BMBF Projekt 17N1111, DOI: 10.2314/GBV:858609622, 2015.
- [9] Pyttel, T., Liebertz, H., Cai, J.: "Failure criterion for laminated glass under impact loading and its application in finite element simulation". International Journal of Impact Engineering, 39, 2012, 252-263.
- [10] Kleuderlein, J., Ensslen, F., Schneider, J.: "Investigation of edge strength dependent on different types of edge processing". engineered transparency. International Conference at glasstec, Düsseldorf, Germany, 2014.
- [11] Weibull, W.: "A statistical theory of the strength of materials". Ingeniörsvetenskapsakademiens Handlingar, 151, 1939, 1–45.
- [12] Frank, T., Kurz, A., Pitzer, M., Söllner, M.: "Development and validation of numerical pedestrian impactor models ". 4th European LS-DYNA Users Conference, 2003, C-II-01/18.
- [13] Du Bois, P.A., Kolling, S., Koesters, M., Frank, T.: "Material behaviour of polymers under impact loading". International Journal of Impact Engineering, 32(5), 2006, 725-740.
- [14] Cicotti, M.: "Stress-corrosion mechanisms in silicate glasses". Journal of Physics D: Applied Physics 42, 2009.
- [15] Manthei, G., Alter, C., Kolling, S.: "Localization of Initial Cracks in Laminated Glass Using Acoustic Emission Analysis–Part I". 31th Conference of the European Working Group on Acoustic Emission (EWGAE), Dresden, 2014.
- [16] Alter, C., Rühl, A., Kolling, S., Schneider, J.: "Experimentelle und numerische Untersuchung des Kopfaufpralls auf Windschutzscheiben". Baustatik-Baupraxis 12, 2014, 291-300.
- [17] Alter, C., Manthei, G., Kolling, S., Schneider, J.: "Lokalisierung des initialen Versagens bei Verbundsicherheitsglas unter stoßartiger Belastung". Stahlbau, 84(S1), 2015, 433-442.